Neuron, Vol. 14, 1233–1246, June, 1995, Copyright © 1995 by Cell Press

Characterization of Spontaneous Calcium Transients in Nerve Growth Cones and Their Effect on Growth Cone Migration

Timothy M. Gomez, Diane M. Snow, and Paul C. Letourneau
University of Minnesota
Department of Cell Biology and Neuroanatomy
Minneapolis, Minnesota 55455

Summary

This study examines the mechanisms of spontaneous and induced $[Ca^{2+}]_i$ spiking in nerve growth cones and the effect of spikes on growth cone migration. Over a 10–20 min observation period, 29% of DRG growth cones undergo spontaneous and transient elevations in physiological extracellular Ca^{2+} ($(Ca^{2+})_o$; 2 mM), whereas 67% of growth cones exposed to 20 mM $(Ca^{2+})_o$ exhibit similar $[Ca^{2+}]_i$ spikes. Spontaneous $[Ca^{2+}]_i$ spiking was not observed in neuronal cell bodies or nonneuronal cells. Ca^{2+} influx through nonvoltage-gated Ca^{2+} channels was required for spontaneous $[Ca^{2+}]_i$ spikes in growth cones, since removal of $(Ca^{2+})_o$, or addition of the general Ca^{2+} channel blockers La^{3+} or Ni^{2+}, reversibly blocked $[Ca^{2+}]_i$ spiking, while blockers of the voltage-gated Ca^{2+} channels did not. Experiments using agents that influence intracellular Ca^{2+} stores suggest that Ca^{2+} stores may buffer and release Ca^{2+} during growth cone $[Ca^{2+}]_i$ spikes. Growth cone migration was immediately and transiently inhibited by $[Ca^{2+}]_i$ spikes, but eventually returned to prespike rates.

Introduction

The complex morphology of adult neurons and the interconnections between neurons and target tissues are dependent in large part on growth cone migration and pathfinding during neural development. Several intracellular second messengers have been implicated as mediators of growth cone migration by extrinsic and intrinsic factors (Mattson et al., 1988b; Bixby, 1989; Lankford and Letourneau, 1991; Letourneau and Cypher, 1991; Lahof et al., 1992; Wu and Goldberg, 1993; Doherty et al., 1994). The best studied second messenger in growth cones is Ca^{2+} (reviewed in Kater and Mills, 1991; Kater et al., 1988). Advance (Suarez-Isla et al., 1984; Mattson and Kater, 1987; Bedlack et al., 1992; Williams et al., 1992) and retraction (Haydon et al., 1984; Cohan and Kater, 1986; Silver et al., 1989; Fields et al., 1990; Bandtlow et al., 1993) of both vertebrate and invertebrate growth cones may be regulated by changes in growth cone intracellular Ca^{2+} concentration ($[Ca^{2+}]_i$). For example, large and sustained increases in the $[Ca^{2+}]_i$ of a growth cone can lead to growth cone collapse by mechanisms thought to involve the disruption of actin filaments (Lankford and Letourneau, 1989). On the other hand, small or transient increases in growth cone $[Ca^{2+}]_i$ can result in more subtle changes in growth cone behavior, such as veil and filopodia protrusion (Goldberg, 1988; Silver et al., 1990; Davenport and Kater, 1992; Rehder and Kater, 1992) and process orientation (Gundersen and Barrett, 1980; Zheng et al., 1994). Therefore, the homeostatic mechanisms controlling the $[Ca^{2+}]_i$ of a growth cone are likely to be important signal transduction processes that regulate growth cone migration following the interactions between cell surface receptors and environmental cues.

A number of Ca^{2+}-regulated systems that influence motility may operate within growth cones. For example, several Ca^{2+}-activated enzymes have been shown to control cytoskeletal organization in other systems. These include proteins associated with the polymerization/depolymerization (Keith et al., 1983; Bengtsson et al., 1993; Rosenmund and Westbrook, 1993), bundling/crosslinking (Sobue and Kanda, 1989), severing/nucleating (Cunningham et al., 1991), and enzymatic degradation (Billger et al., 1988; Shea et al., 1991) of cytoskeletal components (for review, see Stossel et al., 1985). In addition, Ca^{2+} regulates interactions between the cytoskeleton and the plasma membrane (Volberg et al., 1986). Therefore, alteration of growth cone $[Ca^{2+}]_i$ could have multiple effects on cytoskeletal dynamics important for growth cone migration. Ca^{2+} also influences the actin/myosin force-generation system, which may be important in the production of filopodial tension (Letourneau, 1981; Smith, 1988). Thus, filopodial dynamics could be controlled by changes in growth cone $[Ca^{2+}]_i$. Lastly, vesicle fusion to the plasma membrane is controlled by $[Ca^{2+}]_i$ in many systems (reviewed in Augustine et al., 1987). Therefore, changes in $[Ca^{2+}]_i$ may affect polarized membrane insertion necessary for process outgrowth.

$[Ca^{2+}]_i$ transients or oscillations are a common response to agonist activation in many excitable and nonexcitable cells. Several theories have been proposed regarding the advantages of transient versus sustained elevation of cytosolic Ca^{2+} (reviewed in Tsien and Tsien, 1990; Meyer and Stryer, 1991; Fewtrell, 1993). $[Ca^{2+}]_i$ transients may provide a means of triggering effector pathways, while avoiding cell damage that may result from tonic elevation of $[Ca^{2+}]_i$ (Berridge et al., 1988). Consistent with this theory is the finding that the frequency, but not the amplitude, of $[Ca^{2+}]_i$ spikes encodes the strength of agonist stimulation in several cell types (Kuba and Nishi, 1976; Woods et al., 1986). Considering the sensitivity of growth cones to elevated $[Ca^{2+}]_i$ and the number of Ca^{2+}-activated proteins expressed by growth cones, the generation of $[Ca^{2+}]_i$ transients in growth cones could be an important response to activation by extracellular ligands.

Several mechanisms have been proposed to be responsible for $[Ca^{2+}]_i$ spiking (reviewed in Tsien and Tsien, 1990; Meyer and Stryer, 1991; Fewtrell, 1993). $[Ca^{2+}]_i$ transients rely on contributions of Ca^{2+} from extracellular and intracellular sources, by way of Ca^{2+} channels, pumps, exchangers, and binding proteins associated with both the plasma membrane and internal Ca^{2+} stores. Plasma membrane Ca^{2+} channels regulate Ca^{2+} influx from the extracel-

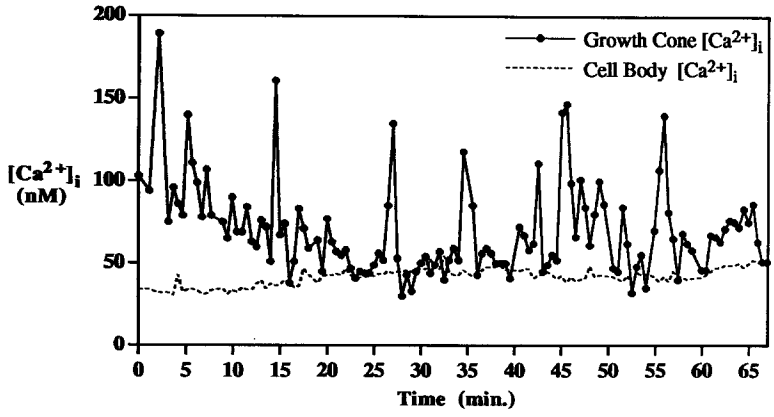

Figure 1. Migrating Chick Neuronal Growth Cones Exhibit Spontaneous $[Ca^{2+}]_i$ Spikes under Normal Conditions In Vitro

The $[Ca^{2+}]_i$ of a growth cone migrating in F14 medium (2 mM $(Ca^{2+})_o$) is plotted every 30 s. Comparison of the $[Ca^{2+}]_i$ of the growth cone with that of a representative cell body, taken from a separate experiment, indicates that growth cone $[Ca^{2+}]_i$ is more dynamically regulated and that $[Ca^{2+}]_i$ spikes periodically occur on top of the dynamic baseline of the growth cone.

lular space and are activated by stimuli such as voltage changes (Fox et al., 1987) and/or extracellular ligands (Benham and Tsien, 1987; Ascher et al., 1988). Intracellular Ca^{2+} stores release Ca^{2+} into the cytosol in response to second messengers, such as inositol trisphosphate (IP_3; Berridge, 1993) and Ca^{2+} itself (Fabiato, 1983). To counteract Ca^{2+} influx and release, several Ca^{2+}-restorative mechanisms, such as Ca^{2+}–ATPase pumps and the Na^+–Ca^{2+} exchanger, extrude Ca^{2+} from the cytosol into internal stores and across the plasma membrane. Alteration in the activity of any component in this system could result in dramatic changes of Ca^{2+} exchange with the cytosol and may thereby lead to $[Ca^{2+}]_i$ transients.

In this study, we examined spontaneous and induced $[Ca^{2+}]_i$ transients in neuronal growth cones. We observed $[Ca^{2+}]_i$ spikes in growth cones and neurites of chick dorsal root ganglia (DRGs), but never in neuronal cell bodies or nonneuronal cells. The goals of the present study were first to characterize $[Ca^{2+}]_i$ spikes in growth cones, then to determine the mechanism by which the spikes were generated, and finally to begin to assess the functional consequences of $[Ca^{2+}]_i$ transients on growth cone behavior.

Results

Characterization of $[Ca^{2+}]_i$ Spikes

$[Ca^{2+}]_i$ Spiking in 2 mM Extracellular Ca^{2+}

Chick DRG growth cones exhibit periodic spontaneous $[Ca^{2+}]_i$ spikes in physiological conditions, i.e., 2 mM extracellular Ca^{2+} ($(Ca^{2+})_o$). Initial experiments conducted in F14 medium indicated that the $[Ca^{2+}]_i$ of growth cones fluctuates more than the $[Ca^{2+}]_i$ of neuronal cell bodies, and that spontaneous $[Ca^{2+}]_i$ spikes periodically occur on top of the dynamic $[Ca^{2+}]_i$ baseline of a growth cone (Figure 1). To prevent the precipitation of polyvalent cations during experimental procedures, growth cones were first shifted into a medium free of all phosphate, carbonate, and sulfate anions (base medium; see Experimental Procedures). Growth cones that were shifted rapidly from F14 medium (containing 2 mM Ca^{2+}) to base medium (containing 2 mM Ca^{2+}) exhibited little change in their baseline $[Ca^{2+}]_i$ (mean increase = 7 ± 4 nM; n = 24) and no increased incidence of spiking. Most experiments were therefore conducted on growth cones that were first shifted to the base medium containing 2 mM Ca^{2+}. $[Ca^{2+}]_i$ transients were observed in 29% of all growth cones followed for up to 20 min while migrating in physiological $(Ca^{2+})_o$ conditions (Figure 2). Therefore, spontaneous $[Ca^{2+}]_i$ spikes appear to be a normal physiological process in migrating DRG growth cones.

Induced $[Ca^{2+}]_i$ Spikes

Elevating the $[Ca^{2+}]_o$ in the bathing medium from 2 to 20

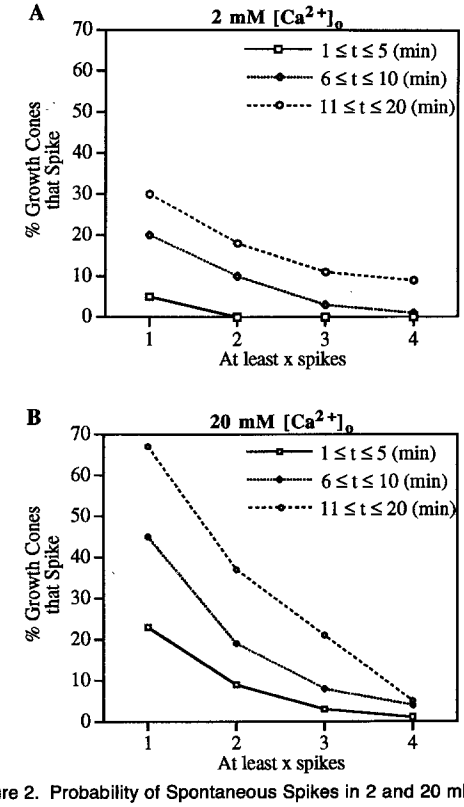

Figure 2. Probability of Spontaneous Spikes in 2 and 20 mM $(Ca^{2+})_o$

Growth cones were observed for variable lengths of time (t = observation period in minutes) while migrating in 2 mM (A) and 20 mM (B) $(Ca^{2+})_o$. Values on the ordinate indicate the least number of $[Ca^{2+}]_i$ spikes exhibited by individual growth cones. The probability of observing 1 or more spontaneous $[Ca^{2+}]_i$ spikes increases in 20 mM $(Ca^{2+})_o$ for all observation periods (n = 338 [2 mM] or 198 [20 mM]).

Table 1. $[Ca^{2+}]_i$ Spike Characteristics

	Baseline $[Ca^{2+}]_i$ (nm)		Spike Amplitude (nM)		Periodicity (min)		Delay to Peak (s)		Duration (s)	
	2 mM $(Ca^{2+})_o$	20 mM $(Ca^{2+})_o$	2 mM $(Ca^{2+})_o$	20 mM $(Ca^{2+})_o$	2 mM $(Ca^{2+})_o$	20 mM $(Ca^{2+})_o$	2 mM $(Ca^{2+})_o$	2 mM $(Ca^{2+})_o$	2 mM $(Ca^{2+})_o$	20 mM $(Ca^{2+})_o$
Growth cone	101 ± 35[a]	142 ± 63[a]	149 ± 58[b]	203 ± 124[b]	8.4 ± 5[c]	9.9 ± 5.2[c]	<20 ± 13[d]	<19 ± 13[d]	<55 ± 21[e]	<48 ± 26[e]
Neurite	ND	ND	100 ± 61[a]	135 ± 96[a]	ND	ND	ND	ND	ND	ND

A comparison of $[Ca^{2+}]_i$ and spike kinetics indicates significant differences in baselines and spike amplitudes for neurons bathed in 2 and 20 mM $(Ca^{2+})_o$. All values are represented as mean ± SD. p values were determined using unpaired Student's t tests. Growth cone $[Ca^{2+}]_i$ spike amplitudes were significantly different in 2 and 20 mM $(Ca^{2+})_o$. In addition, the $[Ca^{2+}]_i$ spike amplitudes of growth cones were significantly greater than those of neurites (10 μm region below base of growth cone) in both 2 and 20 mM $(Ca^{2+})_o$. The time between spikes (periodicity) was determined from only those growth cones that were observed for at least 10 min. Since images were captured at 10 s intervals, delay to peak and spike duration are presented as less than the maximum average time. The true average delay to peak and spike duration may be up to 10 s less than the stated value. Spikes were not observed in cell bodies or nonneuronal cells. However, when shifted from 2 to 20 mM $(Ca^{2+})_o$, cell body and nonneuronal $[Ca^{2+}]_i$ baselines increased from 75 ± 51 nM to 91 ± 70 nM for cell bodies and from 103 ± 60 nM to 114 ± 57 nM for nonneuronal cells. ND, not determined.

[a] $p < .001$.
[b] $p < .002$.
[c] $p < .29$.
[d] $p < .829$.
[e] $p < .295$.

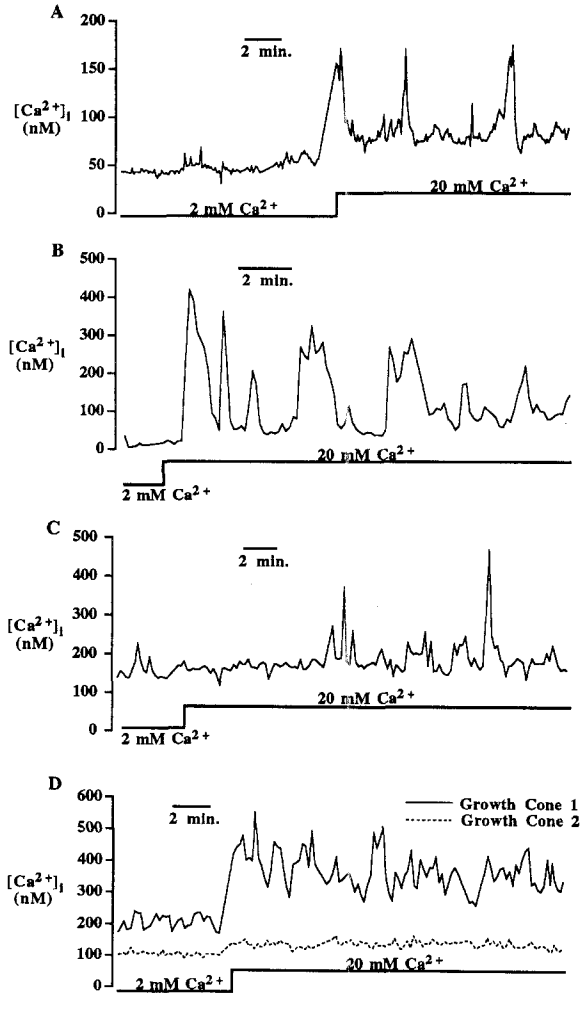

Figure 3. $[Ca^{2+}]_i$ Spiking Patterns Vary among Individual Growth Cones

All growth cones were shifted from 2 to 20 mM $(Ca^{2+})_o$ where indicated by horizontal lines below the graphs. Growth cones 1 and 2 in (D) are from different neurons in the same experiment. Some growth cones begin spiking immediately upon elevation of $(Ca^{2+})_o$ (A and D, growth cone 1), while other growth cones exhibit some delay between the increase in $[Ca^{2+}]_o$ and the first $[Ca^{2+}]_i$ spike (B and C). The frequency, duration, and amplitude of spikes vary between individual growth cones. Some growth cones display only a baseline increase upon elevation of $[Ca^{2+}]_o$ (D, growth cone 2).

mM increased the probability of $[Ca^{2+}]_i$ spiking in growth cones (see Figures 2–6). The longer the observation period and exposure to 20 mM $(Ca^{2+})_o$, the higher the probability of observing a growth cone $[Ca^{2+}]_i$ transient. For all observation periods, the probability of observing a $[Ca^{2+}]_i$ transient more than doubled in 20 mM $(Ca^{2+})_o$ (Figure 2). $[Ca^{2+}]_i$ spiking in growth cones induced by 20 mM $(Ca^{2+})_o$ typically occurred at an elevated $[Ca^{2+}]_i$ baseline and a higher peak amplitude compared with $[Ca^{2+}]_i$ spiking generated in 2 mM $(Ca^{2+})_o$ (Table 1). However, other characteristics of $[Ca^{2+}]_i$ spikes, such as periodicity (i.e., interspike interval), rise time, and duration, were not significantly different for spikes produced in 2 versus 20 mM $(Ca^{2+})_o$ (Table 1). Unlike growth cones, spontaneous $[Ca^{2+}]_i$ spikes were never seen in neuronal cell bodies (see Figure 5D; n = 26; observed an average of 11 min in 20 mM $(Ca^{2+})_o$) or in nonneuronal cells (see Figure 5A; n = 17; observed an average of 9 min in 20 mM $(Ca^{2+})_o$).

The $[Ca^{2+}]_i$ spiking patterns expressed by individual growth cones in 20 mM $(Ca^{2+})_o$ were diverse (Figure 3). For example, some growth cones responded immediately to elevated $(Ca^{2+})_o$ (Figures 3A and 3D, Growth Cone 1), whereas others exhibited a delay between the increase in $[Ca^{2+}]_o$ and the first $[Ca^{2+}]_i$ spike (Figures 3B and 3C). Still other growth cones exhibited only an increased baseline $[Ca^{2+}]_i$ upon elevation of $[Ca^{2+}]_o$ (Figure 3D, Growth Cone 2). These findings suggest that Ca^{2+} is not simply diffusing into a growth cone through a channel of constant permeability, but that a triggered change in a Ca^{2+} homeostatic mechanism(s) may be occurring. Other characteristics of $[Ca^{2+}]_i$ transients such as spike frequency, duration, and amplitude are also variable between growth cones and

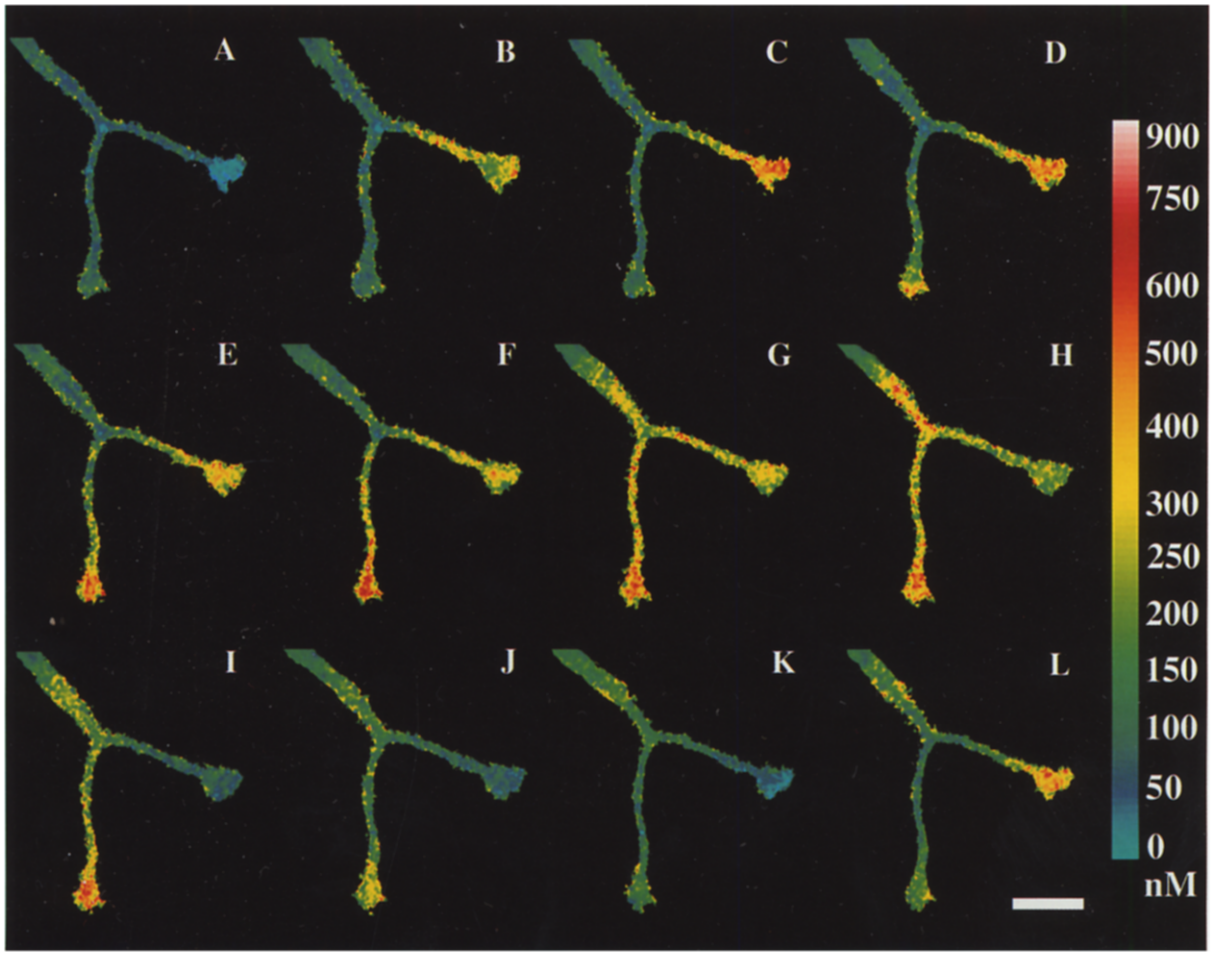

Figure 4. Movement of Elevated $[Ca^{2+}]_i$ within Growth Cones and Neurites

Pseudocolor images depicting $[Ca^{2+}]_i$ are displayed at 10 s intervals. $[Ca^{2+}]_o$ was elevated to 20 mM at 1 min prior to the first image. Spikes appear to originate within each growth cone (lower growth cone in [D]) and pass down the neurites beyond the branch point. The cell body of this neuron was just above the images shown. Bar, 20 μm.

within the same growth cone (Figure 3). Smaller increases in $[Ca^{2+}]_o$ also promoted $[Ca^{2+}]_i$ spiking (see Figure 5A), however with a lower probability.

Movement of Elevated $[Ca^{2+}]_i$ within Growth Cones and Neurites

Growth cones appear to generate $[Ca^{2+}]_i$ transients autonomously; however, elevated $[Ca^{2+}]_i$ can move within neurites, and in branched neurites elevated $[Ca^{2+}]_i$ can pass from one growth cone to another. Figure 4 illustrates $[Ca^{2+}]_i$ spiking in 2 growth cones of a branched neurite. This neuron was shifted to medium containing 20 mM $(Ca^{2+})_o$ at 1 min prior to the first frame. The first $[Ca^{2+}]_i$ spike by this branched neurite was initiated in the growth cone to the right, followed by a spike in the second growth cone beginning 10 s later. A wave of elevated $[Ca^{2+}]_i$ moved down each neurite, past the branch point, and into the parent neurite. Approximately 80 s after the initial rise, the $[Ca^{2+}]_i$ in the right growth cone returned to near baseline, followed shortly after by a drop in the other growth cone. At the end of this sequence, a second $[Ca^{2+}]_i$ transient began in the right growth cone. Although not shown in this short sequence, elevated $[Ca^{2+}]_i$ did appear to pass from one growth cone to another, over a 1 min period later in the sequence. The maximum rate of elevated $[Ca^{2+}]_i$ movement within the neurite was estimated at 22 μm every 10 s, which is consistent with the rate of Ca^{2+} diffusion (Meyer and Stryer, 1991).

Movement of elevated $[Ca^{2+}]_i$ from growth cone to neurite, as shown in Figure 4, occurred in many neurons; however, the distance along a neurite that elevated $[Ca^{2+}]_i$ traveled was variable. For growth cones bathed in either 2 or 20 mM $(Ca^{2+})_o$, the peak amplitude of a $[Ca^{2+}]_i$ spike within a neurite, 10 μm proximal to the base of a growth cone, reached an average of 66% ± 42% of the peak $[Ca^{2+}]_i$ spike within the growth cone (Table 1). In some neurons, elevated $[Ca^{2+}]_i$ occurred >50 μm down the neurite (Figure 4), whereas other spikes were not propagated beyond the growth cone. Typically $[Ca^{2+}]_i$ transients were initiated within the growth cone, but in some instances the $[Ca^{2+}]_i$ rise appeared first within the neurite (7 of 125 cases). These results suggest that $[Ca^{2+}]_i$ spikes are generated in the growth cone or neurite, independently of the cell

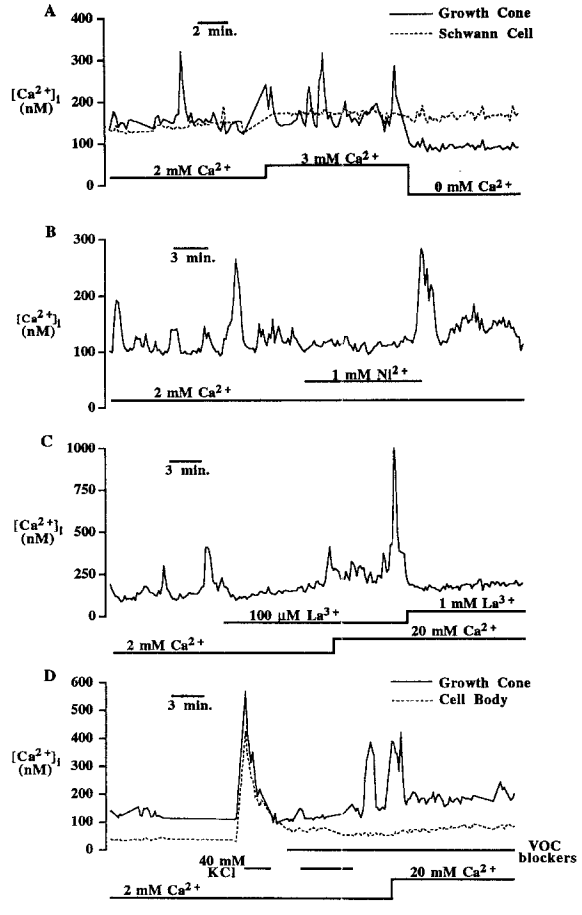

Figure 5. $[Ca^{2+}]_i$ Transients Are Dependent on Ca^{2+} Influx through a Non-Voltage-Gated Channel(s)

In all graphs, changes in bathing solutions are indicated by horizontal lines below the graphs.

(A) Elevating the $[Ca^{2+}]_o$ to 3 mM has little effect on growth cone $[Ca^{2+}]_i$ transients; however, spikes immediately stop when medium is changed to nominally Ca^{2+}-free. Nonneuronal cells do not exhibit $[Ca^{2+}]_i$ transients and undergo little change in baseline $[Ca^{2+}]_i$ with changes in the $[Ca^{2+}]_o$.

(B) Ni^{2+} (1 mM) reversibly blocks $[Ca^{2+}]_i$ spiking in 2 mM $(Ca^{2+})_o$.

(C) La^{3+} (100 μM) inhibits $[Ca^{2+}]_i$ spiking in 2 mM $(Ca^{2+})_o$; however, 1 mM La^{3+} is required to inhibit spiking in 20 mM $(Ca^{2+})_o$.

(D) Blockers to the N-, L-, and T-type voltage-operated Ca^{2+} channels (VOC blockers; see text for details) inhibit $[Ca^{2+}]_i$ transients in both cell bodies and growth cones elicited with 40 mM K^+, but do not block spontaneous $[Ca^{2+}]_i$ transients in 2 or 20 mM $(Ca^{2+})_o$.

body. The finding that $[Ca^{2+}]_i$ transients are propagated a variable distance down a neurite and are occasionally initiated within a neurite suggests that, to different degrees, neurites and growth cones possess similar mechanisms for generating $[Ca^{2+}]_i$ transients.

Small local hot spots of elevated $[Ca^{2+}]_i$ were also apparent in many growth cones and neurites during $[Ca^{2+}]_i$ transients (Figure 4). The $[Ca^{2+}]_i$ in these regions often exceeded 1 μM, but owing to their small size, no further quantitative analysis was performed on them.

Mechanisms of $[Ca^{2+}]_i$ Spiking

Role of Ca^{2+} Influx

$(Ca^{2+})_o$ is required for both the generation and maintenance of $[Ca^{2+}]_i$ spikes in growth cones. Removing $(Ca^{2+})_o$ stopped $[Ca^{2+}]_i$ spiking in all growth cones examined (12 growth cones from 7 experiments) and lowered the baseline $[Ca^{2+}]_i$ to a stable, steady-state level (Figure 5A). Typically, it took 20–30 s after the removal of $(Ca^{2+})_o$ to begin imaging a growth cone again. With this delay, we observed only 1 growth cone undergo 1 $[Ca^{2+}]_i$ spike in the absence of $(Ca^{2+})_o$; this spike occurred several minutes after the removal of $(Ca^{2+})_o$, presumably owing to the release of Ca^{2+} from intracellular stores. Therefore, Ca^{2+} influx plays an important and possibly dominant role in the generation of $[Ca^{2+}]_i$ transients in growth cones.

Polyvalent cations such as Ni^{2+} and La^{3+} are used as general Ca^{2+} channel blockers in combination with Fura 2 Ca^{2+} imaging (Schilling et al., 1989; Clementi et al., 1992; Demaurex et al., 1992; Laskey et al., 1992). These blockers compete with Ca^{2+} for access to the channel pore, and in some cases they may permeate Ca^{2+} channels. Since both Ni^{2+} and La^{3+} will bind Fura 2 and alter its fluorescent properties, we first determined whether these ions permeate growth cones to an extent that would confound $[Ca^{2+}]_i$ measurements during their use as Ca^{2+} channel blockers. The association of Ni^{2+} with Fura 2 in a cell-free solution quenches fluorescence emissions at all excitation wavelengths (Shibuya and Douglas, 1992; and our unpublished data using Fura 2 salt in cell-free solutions). However, in no instance were Fura 2 emissions quenched in growth cones exposed to up to 10 mM Ni^{2+}. Furthermore, shifts in the intracellular Fura 2 emission ratio, in the presence of extracellular Ni^{2+}, were the result of appropriate 350 and 380 nm wavelength changes. Therefore, Ni^{2+} does not appear to enter growth cones and confound its use as a Ca^{2+} channel blocker in combination with Fura 2 Ca^{2+} imaging. On the other hand, the binding of La^{3+} to Fura 2 increases the 350:380 emission ratio just as Ca^{2+} does (unpublished data using Fura 2 salt in cell-free solutions). However, in intact melanotrophs, an increased Fura 2 emission ratio in response to La^{3+} appears to be irreversible (Shibuya and Douglas, 1992), suggesting that upon entering cells La^{3+} cannot be extruded or irreversibly binds Fura 2. Therefore, entry of La^{3+} into growth cones would result in an apparent, irreversible $[Ca^{2+}]_i$ baseline increase. Consistent with this notion, the addition of up to 1 mM La^{3+} sometimes caused slow, steady, and irreversible Fura 2 ratio increases in growth cones (Figure 5C). However, these minor increases in the apparent $[Ca^{2+}]_i$ baseline did not affect subsequent $[Ca^{2+}]_i$ transients, suggesting that La^{3+} enters growth cones gradually, but does not significantly affect the determination of $[Ca^{2+}]_i$ changes over the time course over which we used this blocker. Therefore, when used with caution, La^{3+} also appears to be a valid Ca^{2+} channel blocker in combination with Fura 2 Ca^{2+} imaging.

Ions that block Ca^{2+} channels inhibit $[Ca^{2+}]_i$ spiking in the presence of $(Ca^{2+})_o$, but only if the ratio of the concentration of $(Ca^{2+})_o$ to that of the channel-blocking ion ex-

ceeds a threshold level. Spontaneous $[Ca^{2+}]_i$ transients in 2 mM $(Ca^{2+})_o$ (Figure 5B; n = 16), but not in 20 mM $(Ca^{2+})_o$ (data not shown; n = 7), were blocked by 1 mM Ni^{2+}. Similarly, 100 μM La^{3+} effectively blocked $[Ca^{2+}]_i$ spiking in 2 mM $(Ca^{2+})_o$ (Figure 5C; n = 6), but at least 1 mM La^{3+} was required to inhibit $[Ca^{2+}]_i$ spiking in 20 mM $(Ca^{2+})_o$ (Figure 5C; n = 9). These results confirm that Ca^{2+} competes with other cations for access to the plasma membrane channels. Active feedback control of $[Ca^{2+}]_i$ is indicated by the immediate and transient rise in $[Ca^{2+}]_i$ that often occurred upon removal of the channel-blocking agent (Figure 5B). Such a feedback mechanism may reflect Ca^{2+}-dependent stimulation of a Ca^{2+}–ATPase and/or a Ca^{2+}-induced inhibition of an influx pathway. Although these results demonstrate a need for Ca^{2+} influx in the initiation and maintenance of $[Ca^{2+}]_i$ spikes, they do not indicate which Ca^{2+} channels are involved.

$[Ca^{2+}]_i$ transients generated by Ca^{2+} influx through voltage-sensitive channels have been described in a number of other systems (reviewed in Tsien et al., 1988; Bean, 1989). To determine whether voltage-sensitive Ca^{2+} currents are necessary for $[Ca^{2+}]_i$ spiking in growth cones, we blocked the N-, L-, and T-type Ca^{2+} channels, which are the predominant voltage-gated channels of DRGs (Fox et al., 1987), and tested for an effect on spontaneous $[Ca^{2+}]_i$ transients. A cocktail consisting of 1 μM Ω-conotoxin, 10 μM verapamil, 100 nM nifedipine, and 50 μM Ni^{2+} was first tested for its ability to inhibit depolarization-dependent Ca^{2+} influx. Blocking the N-, L-, and T-type voltage-sensitive Ca^{2+} channels completely suppressed depolarization-dependent Ca^{2+} entry into growth cones and cell bodies (Figure 5D; n = 8), suggesting that these are the predominant voltage-sensitive Ca^{2+} channels expressed on DRG cell bodies and growth cones. In contrast, in no case did blocking voltage-gated Ca^{2+} channels inhibit the generation of spontaneous growth cone $[Ca^{2+}]_i$ spikes in 2 or 20 mM $(Ca^{2+})_o$ (Figure 5D; n = 6). Additionally, $[Ca^{2+}]_i$ spikes were also observed in the presence of 60 nM Ω-agatoxin IVA, a P-type voltage-gated Ca^{2+} channel blocker (n = 3) and 1 μM tetrodotoxin (n = 2; both generous gifts of Dr. S. Thayer, University of Minnesota). These findings suggest that Ca^{2+} influx into a growth cone during $[Ca^{2+}]_i$ transients occurs primarily through a non-voltage-gated Ca^{2+}-channel(s), and that membrane voltage changes are not responsible for $[Ca^{2+}]_i$ spikes in growth cones. The identity of this Ca^{2+} entry pathway is presently unknown.

Role of Intracellular Ca^{2+} Stores and Pumps

We tested for the presence of intracellular Ca^{2+} storage organelles in growth cones by exposing them to thapsigargin (TG) and the structurally dissimilar cyclopiazonic acid (CPA), which are inhibitors of Ca^{2+}–ATPase activity associated with endoplasmic and sarcoplasmic reticulum, respectively (Seidler et al., 1989; Thastrup et al., 1990). TG (irreversible) and CPA (slowly reversible) have been shown to mobilize Ca^{2+} specifically from IP_3-sensitive Ca^{2+} stores (Foskett and Wong, 1992), presumably by inhibiting Ca^{2+} sequestration into these pools, leading to store depletion by a persistent Ca^{2+} leak. We tested for the presence of TG/CPA-releasable Ca^{2+} storage organelles by exposing growth cones in Ca^{2+}-free medium (1 mM EGTA) to 1 μM TG or 30 μM CPA. In the absence of $(Ca^{2+})_o$, TG and CPA increased the $[Ca^{2+}]_i$ in 75% of growth cones tested (Figure 6A; peak release = 59 ± 49 nM over 3.4 ± 2.9 min; n = 12). Interestingly, TG/CPA-sensitive stores are not the only Ca^{2+} pools within growth cones, since large ionomycin-releasable stores are still intact within growth cones, even after exposure to TG or CPA, in the continued absence of $(Ca^{2+})_o$ (Figure 6A).

To determine whether IP_3-sensitive Ca^{2+} stores are required for the generation of $[Ca^{2+}]_i$ spikes in growth cones, we depleted these pools, in Ca^{2+}-containing media, using TG or CPA. Addition of 1 μM TG or 30 μM CPA to growth cones spontaneously spiking in 2 or 20 mM $(Ca^{2+})_o$ did not block $[Ca^{2+}]_i$ transients (7 of 11 growth cones spiked during observation period following addition of TG or CPA; Figure

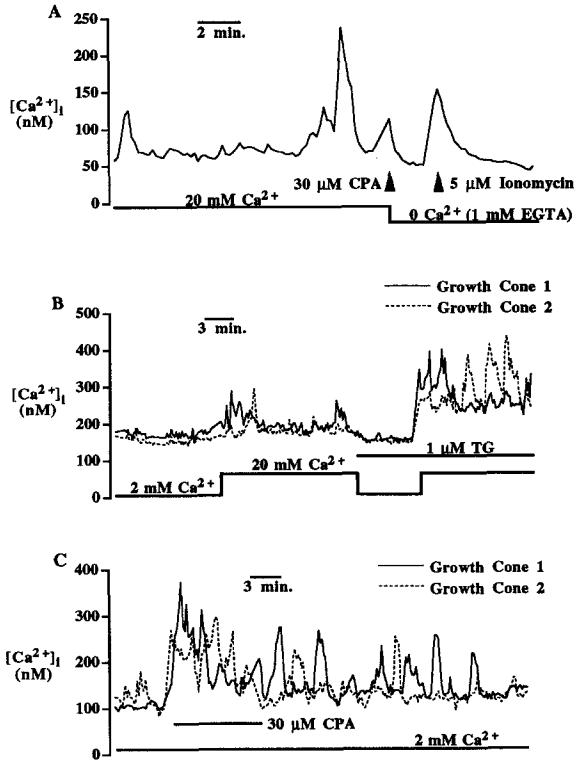

Figure 6. Inhibition of Ca^{2+}–ATPases That Refill Intracellular Ca^{2+} Stores Potentiates $[Ca^{2+}]_i$ Spiking in Growth Cones When $(Ca^{2+})_o$ Is Present

(A) A growth cone that was spiking in 20 mM $(Ca^{2+})_o$ was exposed to 30 μM CPA in the absence of $(Ca^{2+})_o$. CPA (applied at first arrowhead) elicits a small biphasic $[Ca^{2+}]_i$ rise in Ca^{2+}-free media, indicating that Ca^{2+} has been released from intracellular stores. A second release of Ca^{2+} can be elicited by ionomycin (second arrowhead), in the continued absence of $(Ca^{2+})_o$, suggesting that additional stores are present.

(B) Two growth cones from the same neuron were shifted from 2 to 20 mM $(Ca^{2+})_o$, both in the absence and in the presence of 1 μM TG. $[Ca^{2+}]_i$ transients are of greater amplitude in 20 mM $(Ca^{2+})_o$ with TG present.

(C) Brief application of CPA, a slowly reversible Ca^{2+}–ATPase inhibitor, induced long-lasting $[Ca^{2+}]_i$ spikes in 2 growth cones of a branched neurite that were bathed continuously in 2 mM $(Ca^{2+})_o$.

6B). To the contrary, TG and CPA induced robust $[Ca^{2+}]_i$ spiking in 36% of growth cones that were not spiking prior to TG or CPA addition (Figure 6C; n = 33). Furthermore, the mean peak amplitude of growth cone $[Ca^{2+}]_i$ transients was significantly greater after exposure to TG or CPA in both 2 and 20 mM $(Ca^{2+})_o$ (cf. Table 1; peak amplitude in 2 mM $(Ca^{2+})_o$ with TG or CPA = 197 ± 74 nM [$p < .03$; n = 10]; peak amplitude in 20 mM $(Ca^{2+})_o$ with TG or CPA = 302 ± 160 nM [$p < .02$; n = 9]; Figure 6B). Since the IP_3-sensitive Ca^{2+} stores remain continuously depleted during TG and CPA treatments (Foskett et al., 1991), these pools are not likely to be involved in the generation of $[Ca^{2+}]_i$ transients. The apparent enhancement of $[Ca^{2+}]_i$ spiking in growth cones by blocking the refilling of the IP_3-sensitive Ca^{2+} stores suggests that these Ca^{2+} stores normally buffer $[Ca^{2+}]_i$ transients in growth cones.

$[Ca^{2+}]_i$ Spiking Is Caffeine Sensitive

$[Ca^{2+}]_i$ spiking in some cell types has been attributed to Ca^{2+}-induced Ca^{2+} release (CICR), in which Ca^{2+} influx induces Ca^{2+} release from intracellular organelles through a ryanodine-, caffeine-, and cADP ribose–sensitive channel, termed the ryanodine receptor (Fabiato, 1983; Hua et al., 1994). Caffeine is believed to modulate or induce Ca^{2+} release through this channel by lowering the sensitivity of the channel to release by endogenous Ca^{2+} and cADP ribose (Rousseau and Meissner, 1989; Lee, 1993). Caffeine generates $[Ca^{2+}]_i$ spiking in many cell types by activating the ryanodine receptor (Kuba and Nishi, 1976; Wakui et al., 1990; Friel and Tsien, 1992); however, caffeine has also been shown to modulate $[Ca^{2+}]_i$ by inhibiting phosphodiesterases (Neyses et al., 1985) and by directly inhibiting Ca^{2+} influx (Lipscombe et al., 1988a; Martin et al., 1989; Hughes et al., 1990; Noack et al., 1990; Nohmi et al., 1992).

We used a similar experimental paradigm as described above to test for the presence of caffeine-releasable Ca^{2+} storage organelles in growth cones. In contrast to release from the IP_3-sensitive stores, but consistent with previous findings (Lipscombe et al., 1988b; Thayer et al., 1988b), 10 mM caffeine stimulated a small and more transient $[Ca^{2+}]_i$ increase in only 23% of growth cones tested (Figure 7A; peak release = 38 ± 28 nM over <1 min; n = 13). Furthermore, a second Ca^{2+} release, in the continued absence of $(Ca^{2+})_o$, could often be elicited with Ca^{2+}–ATPase inhibitors after exposure to caffeine (Figure 7A). Therefore, caffeine-releasable stores are likely to be a subset of the CPA/TG-sensitive Ca^{2+} stores and in only a subpopulation of DRG growth cones. Again, the large ionomycin-releasable source of Ca^{2+} is still present within growth cones, even after stimulation with caffeine and CPA (Figure 7A). This ionomycin-releasable source of Ca^{2+} is not likely to be mitochondrial, since under similar conditions no changes in $[Ca^{2+}]_i$ were observed in response to the mitochondrial poison FCCP (data not shown). Therefore, growth cones appear to possess multiple types of Ca^{2+} storage organelles, some of which are not released by caffeine or CPA/TG.

Despite the low percentage of growth cones that possess caffeine-releasable intracellular Ca^{2+} stores, we tested the effect of caffeine on $[Ca^{2+}]_i$ spiking in growth cones. We found that caffeine potentiated spontaneous $[Ca^{2+}]_i$ spiking in a subset of growth cones bathed in 20 mM $(Ca^{2+})_o$ (Figure 7B). Potentiation of spontaneous $[Ca^{2+}]_i$ spiking was indicated by a decreased interspike interval. The most obvious elevation of spike frequency occurred

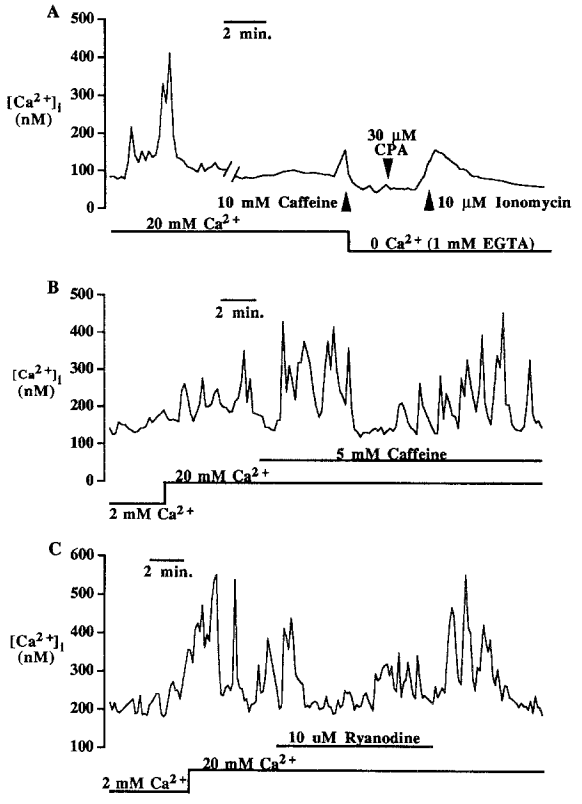

Figure 7. Caffeine and Ryanodine Have Opposite Effects on $[Ca^{2+}]_i$ Spiking in Growth Cones

(A) A growth cone that was spiking in 20 mM $(Ca^{2+})_o$ was exposed to 10 mM caffeine simultaneously with removing $(Ca^{2+})_o$. The break in the graph represents an 18 min period when no spikes occurred. Caffeine (applied at first arrowhead) elicits a small biphasic $[Ca^{2+}]_i$ rise in Ca^{2+}-free media, indicating that Ca^{2+} has been released from intracellular stores. Subsequent application of CPA (second arrowhead), in Ca^{2+}-free media, often induces a second biphasic $[Ca^{2+}]_i$ rise. Release of Ca^{2+} by CPA following caffeine treatment was seen in several growth cones (data not shown), suggesting that caffeine-releasable stores make up a subset of, or are distinct from, CPA-releasable stores in growth cones. Furthermore, in the continued absence of $(Ca^{2+})_o$, after exposure to both caffeine and CPA, large ionomycin-releasable Ca^{2+} stores (ionomycin applied at third arrowhead) still exist within this growth cone.

(B) A growth cone that exhibits small $[Ca^{2+}]_i$ spikes in 20 mM $(Ca^{2+})_o$ begins robust spiking shortly after exposure to 5 mM caffeine.

(C) Ryanodine reversibly decreases $[Ca^{2+}]_i$ spike amplitude. Addition of 10 μM ryanodine to a growth cone exhibiting large $[Ca^{2+}]_i$ transients reduces spike amplitude, but does not completely block spikes. The single large spike shortly after the addition of ryanodine is consistent with the use dependence or slow association kinetics of this drug (Thayer et al., 1988a). $[Ca^{2+}]_i$ spikes return to pretreatment amplitude immediately upon removal of ryanodine. The mean peak spike amplitude for 6 growth cones prior to ryanodine treatment (312 nM) was significantly greater than that during ryanodine treatment (150 nM; $p < .001$, paired t test).

in 21% (n = 28) of growth cones exposed to 5 or 10 mM caffeine in 20 mM $(Ca^{2+})_o$ (mean spike period = 2.7 ± 1.5; n = 6; $p < .002$). Although not directly tested, the population of growth cones stimulated by caffeine may be the same as that found to possess caffeine-releasable intracellular Ca^{2+} stores (see above).

As a caveat, spontaneous $[Ca^{2+}]_i$ transients in growth cones were apparently inhibited by caffeine when the concentration of caffeine exceeded $[Ca^{2+}]_o$ by a threshold level (2.5- to 5-fold; n = 50). However, we believe the caffeine-induced inhibition of $[Ca^{2+}]_i$ spiking in growth cones to be an artifact due to physical effects of caffeine on Fura 2 fluorescence. Similar to the findings of Nohmi et al. (1992), we found that, in a concentration-dependent manner, caffeine increased the fluorescence of cell-free Fura 2 salt (see Experimental Procedures) at all excitation wavelengths. However, caffeine increased Fura 2 emissions at longer excitation wavelengths more than it increased emissions at shorter ones (380 > 360 > 350), resulting in a drop in the 350:380 emission ratio, which would predict a lower $[Ca^{2+}]_i$. Furthermore, 50 mM caffeine attenuated ratio increases induced by increasing $[Ca^{2+}]_o$. These results indicate that Ca^{2+} imaging using Fura 2 on our apparatus may be compromised in the presence of a high concentration of caffeine, and that $[Ca^{2+}]_i$ spiking observed in a lower concentration of caffeine may be more pronounced than indicated.

$[Ca^{2+}]_i$ Spiking Is Ryanodine Sensitive

Lastly, the plant alkaloid ryanodine is a drug that binds with high specificity to the Ca^{2+} release channel in brain and muscle thought to be responsible for CICR (Imagawa et al., 1987; McPherson et al., 1991). Ryanodine is believed to inhibit CICR by locking channels into completely closed or subconducting states, leading to store depletion (Lai et al., 1989). We applied 1 or 10 μM ryanodine to growth cones spiking in 2 and 20 mM $(Ca^{2+})_o$ and found that ryanodine reversibly attenuated $[Ca^{2+}]_i$ spike amplitude in all growth cones tested (Figure 7C; n = 6). The reduction in spike amplitude is consistent with the notion that $[Ca^{2+}]_i$ spikes in growth cones are driven by Ca^{2+} influx, but may be amplified by release of Ca^{2+} from Ca^{2+}-sensitive stores. It is unclear why all growth cones responded to ryanodine when only a small percentage responded to caffeine; however, this may indicate the presence caffeine-insensitive ryanodine receptors in growth cones (Giannini et al., 1992).

Effect of $[Ca^{2+}]_i$ Spiking on Growth Cone Behavior

The occurrence of a $[Ca^{2+}]_i$ spike is associated with a decrease in the rate of growth cone migration. This was demonstrated by comparing the mean distance migrated during three 5 min periods: immediately before, immediately after, and 5–10 min after the peak of a $[Ca^{2+}]_i$ transient (Figure 8). The average distance migrated was significantly less during the first 5 min after a spontaneous spike than during the 5 min period before the peak of the $[Ca^{2+}]_i$ transient (Figure 8B). Between 5 and 10 min after the peak of a $[Ca^{2+}]_i$ spike, the mean distance migrated increased to approach the prespike level (Figure 8). The prespike migration rate was not different from the mean migration rate during 5 min periods not associated with a $[Ca^{2+}]_i$ spike as defined above. This suggests that changes in growth cone migration were an effect of a $[Ca^{2+}]_i$ spike, not a cause. Although not quantified, the spike amplitude and duration appeared to correlate with the extent to which growth cone migration slowed (Figure 8A).

In a separate set of experiments, the rate of neurite outgrowth was determined before and after a shift from 2 to 20 mM $(Ca^{2+})_o$, while monitoring growth cone migration with time-lapse phase-contrast microscopy only. Growth cones were recorded for at least 1 hr in 2 mM $(Ca^{2+})_o$, then for at least 1 hr more after switching to 20 mM $(Ca^{2+})_o$. Neurites elongated an average of 0.60 ± 0.2 μm/min in

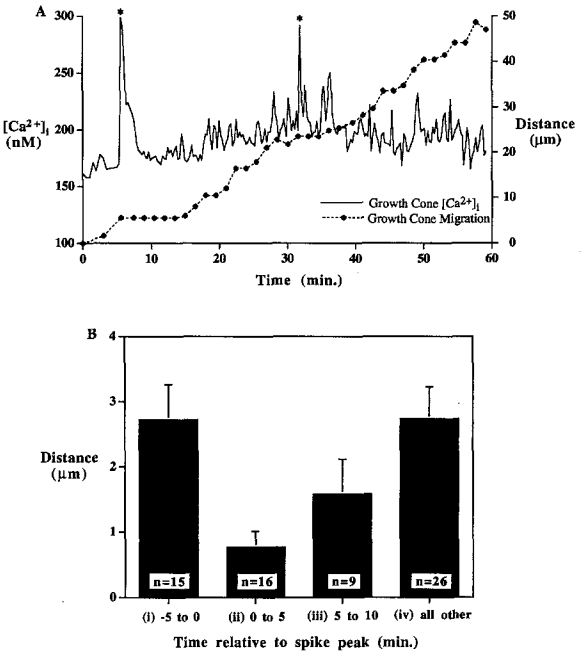

Figure 8. $[Ca^{2+}]_i$ Spikes Decrease the Rate of Growth Cone Migration

(A) The $[Ca^{2+}]_i$ and distance migrated over time are plotted for a growth cone migrating in 2 mM $(Ca^{2+})_o$. Two $[Ca^{2+}]_i$ transients that exceeded the baseline $[Ca^{2+}]_i$ by at least 100 nM (indicated by asterisk) are each associated with an immediate reduction in the rate of migration that lasts for several minutes before returning to the prespike level.

(B) Determination of growth cone migration during 5 min periods before and after $[Ca^{2+}]_i$ spikes (mean ± SEM). Growth cone migration was separated into four periods of 5 min each. The periods included: 5 min immediately before the spike peak (i), 5 min immediately after the spike peak (ii), 5–10 min after the spike peak (iii), and all other 5 min periods that did not overlap any of the first three (iv). A total of 16 spikes from 9 growth cones in both 2 and 20 mM $(Ca^{2+})_o$ were analyzed in this way; 5 growth cones were bathed continuously in 2 mM $(Ca^{2+})_o$, and 4 growth cones were shifted into 20 mM $(Ca^{2+})_o$. In some instances, the growth cone was not observed for a full 5 min before or after the spike peak, in which case that period was excluded from the data set. The distance migrated by growth cones was significantly less in the 5 min period after the peak of a $[Ca^{2+}]_i$ spike (ii) than in the 5 min before (i; $p < .005$). The mean distance migrated 5–10 min after the spike peak (iii) increased but was not significantly different compared with the distance migrated immediately after the spike peak ($p = .126$), or compared with any other 5 min period. The distance migrated by growth cones during all other 5 min periods (iv) was also significantly greater than the distance migrated immediately following a $[Ca^{2+}]_i$ transient (ii; $p < .005$), but was not significantly different from the 5 min prespike periods (i).

2 mM $(Ca^{2+})_o$, but the elongation rate dropped to 0.20 ± 0.2 μm/min in 20 mM $(Ca^{2+})_o$ ($p < .0001$, paired t test; $n = 19$). Although $[Ca^{2+}]_i$ was not monitored in these experiments, these results are consistent with the findings that $[Ca^{2+}]_i$ transients are more frequent in 20 mM $(Ca^{2+})_o$, and that spikes are associated with a decreased rate of neurite outgrowth. However, high $[Ca^{2+}]_o$ may affect growth cone migration by processes that are independent of an increased frequency and amplitude of $[Ca^{2+}]_i$ spikes.

Discussion

We have used high resolution video imaging of Fura 2 fluorescence to show that migrating chick DRG growth cones exhibit spontaneous transient elevations in $[Ca^{2+}]_i$ in vitro. $[Ca^{2+}]_i$ spikes were initiated primarily within growth cones; however, elevated $[Ca^{2+}]_i$ traveled variable distances down neurites. These $[Ca^{2+}]_i$ transients were initiated by Ca^{2+} influx through a non-voltage-gated channel(s) that was blocked by high levels of Ni^{2+} and La^{3+}. Furthermore, release of Ca^{2+} from TG- or CPA-sensitive intracellular stores was not required for $[Ca^{2+}]_i$ transients. Instead, these stores may buffer rapid changes in $[Ca^{2+}]_i$. Amplification of $[Ca^{2+}]_i$ transients by release of Ca^{2+} from intracellular stores may occur in a subset of growth cones, since caffeine and ryanodine altered $[Ca^{2+}]_i$ spiking in some cases. Autonomous $[Ca^{2+}]_i$ transients in nerve growth cones were associated with decreases in the rate of growth cone migration.

Characterization of $[Ca^{2+}]_i$ Spikes

The spatial and temporal regulation of $[Ca^{2+}]_i$ was more dynamic within neuronal processes, as compared with cell bodies and nonneuronal cells. The baseline $[Ca^{2+}]_i$ normally fluctuated more in growth cones than in neurites or cell bodies, and $[Ca^{2+}]_i$ spikes commonly occurred within growth cones. Furthermore, altering the $[Ca^{2+}]_o$ had a greater effect on the baseline $[Ca^{2+}]_i$ and on the incidence of $[Ca^{2+}]_i$ spikes in growth cones. What properties expressed by growth cones underlie such dramatic differences in their regulation of $[Ca^{2+}]_i$?

The flat morphology of growth cones is one characteristic that distinguishes them from neuronal cell bodies. The high surface to volume ratio of growth cones may be one important factor contributing to their very dynamic $[Ca^{2+}]_i$; however, it is not likely to be the only distinguishing characteristic, since nonneuronal cells (Schwann cells and fibroblasts), which do not exhibit spontaneous $[Ca^{2+}]_i$ transients, also have higher surface to volume ratios than neuronal perikarya. Therefore, growth cones likely express unique Ca^{2+}-homeostatic systems.

The kinetics of $[Ca^{2+}]_i$ spikes in growth cones suggest that they are generated by influx of extracellular Ca^{2+}. The mean rise time of $[Ca^{2+}]_i$ spikes was nearly 20 s in both 2 mM and 20 mM $(Ca^{2+})_o$, and the duration of spikes was just under 1 min (Table 1). These rates are considerably longer than would be expected if spikes were generated by intracellular Ca^{2+} release in response to either IP_3 or Ca^{2+} (CICR) (Meyer and Stryer, 1991). Interestingly, $[Ca^{2+}]_i$ spikes of similar rise time and duration have been identified in other cell types (Lewis and Cahalan, 1989; Kojima et al., 1992; Laskey et al., 1992), where it was concluded that the spikes were generated by Ca^{2+} influx. In view of the large surface of plasma membrane, it is not surprising that Ca^{2+} influx is critical to spiking in growth cones.

Regional analysis of elevated $[Ca^{2+}]_i$ indicates that Ca^{2+} travels from growth cones into neurites to varying degrees. During a growth cone $[Ca^{2+}]_i$ transient, the average $[Ca^{2+}]_i$ elevation within a neurite, 10 μm proximal to the growth cone, was 66% ± 42% of the growth cone level (Table 1). The reduced spike amplitude and high variability of Ca^{2+} movement suggest that elevated $[Ca^{2+}]_i$ normally diminishes within neurites. However, $[Ca^{2+}]_i$ can reach an equal or even greater level in some neurites, punctuated by the observation that $[Ca^{2+}]_i$ spikes in 5.6% of neurons were initiated within a neurite. These results suggest that the cellular machinery underlying $[Ca^{2+}]_i$ spikes is unequally distributed along processes and may vary between neurons.

$[Ca^{2+}]_i$ Spikes Are Dependent upon Ca^{2+} Influx

We conclude that Ca^{2+} influx is required for $[Ca^{2+}]_i$ spiking in growth cones, because rapid removal of $(Ca^{2+})_o$ or addition of channel-blocking cations immediately stopped spiking. In addition, growth cones shifted from 2 to 20 mM $(Ca^{2+})_o$ displayed an elevated $[Ca^{2+}]_i$ baseline and a greater probability of $[Ca^{2+}]_i$ spikes, which were of a higher peak amplitude, but similar duration and frequency (Table 1). The elevated peak spike amplitude and baseline $[Ca^{2+}]_i$ in 20 mM $(Ca^{2+})_o$ reflect an increased force driving Ca^{2+} into the growth cone and further indicate that influx dominates $[Ca^{2+}]_i$ transients.

The increased incidence of $[Ca^{2+}]_i$ spiking in 20 mM $(Ca^{2+})_o$ (see Figure 2) may reflect Ca^{2+}-dependent regulation of Ca^{2+} influx or efflux by a negative feedback mechanism, as suggested for other cell types exhibiting $[Ca^{2+}]_i$ oscillations (Lewis and Cahalan, 1989). In support of this notion is the observation that spikes often occurred immediately upon elevation of $(Ca^{2+})_o$ (see Figures 3A and 3D), or after the removal of a channel-blocking cation (see Figure 5B). Feedback control of Ca^{2+} entry could be due to inhibition of an influx pathway or activation of a Ca^{2+} extrusion pump following a $[Ca^{2+}]_i$ rise in response to increased force driving Ca^{2+} into a growth cone. Interestingly, some investigators report that Ca^{2+} channel conductances are activated upon elevation of $[Ca^{2+}]_i$ (Marban and Tsien, 1982; Gurney et al., 1989; Friel and Tsien, 1992), whereas others report they are inhibited (Brehm and Eckert, 1978; Lewis and Cahalan, 1989). These findings suggest an intriguing possibility, that $[Ca^{2+}]_i$ transients in growth cones arise by Ca^{2+} influx through plasma membrane channels that are regulated in a similar manner as CICR through ryanodine receptors (Fabiato, 1983). Because blockers of the voltage-operated Ca^{2+} channels do not inhibit $[Ca^{2+}]_i$ spikes, we propose that Ca^{2+} enters growth cones through non-voltage-gated channels during spontaneous transients.

Role of Intracellular Ca^{2+} Stores

In many cell types, Ca^{2+} influx is the first step in a process that stimulates Ca^{2+} release from intracellular organelles (reviewed in Tsien and Tsien, 1990; Meyer and Stryer, 1991; Fewtrell, 1993). One model proposes that $[Ca^{2+}]_i$ spikes depend on the repetitive release and reuptake of Ca^{2+} from organelles in response to elevated $[Ca^{2+}]_i$ (Kuba and Takeshita, 1981). Release-dependent $[Ca^{2+}]_i$ spikes are clearly demonstrated by the persistence of spikes for one or more cycles after removal of $(Ca^{2+})_o$, and by stimulation or inhibition of transients by agents that activate the channels responsible for Ca^{2+} release from intracellular organelles. Based on these criteria, $[Ca^{2+}]_i$ spikes in chick DRG growth cones do not require release of Ca^{2+} from intracellular stores. $[Ca^{2+}]_i$ spikes were not observed in nominally Ca^{2+}-free medium or in the presence of general Ca^{2+} channel blockers. Enhancement of $[Ca^{2+}]_i$ spiking by caffeine occurred in a small percentage of growth cones (see Figure 7B). Ryanodine, a blocker of CICR, attenuated but did not completely block spiking (see Figure 7C). The inconsistent responses of growth cones to caffeine and ryanodine indicate that Ca^{2+} release may contribute to $[Ca^{2+}]_i$ transients in some growth cones, but that Ca^{2+} influx is the primary contributor to $[Ca^{2+}]_i$ spikes in most growth cones.

Three observations support the possibility that $[Ca^{2+}]_i$ spikes in growth cones could be amplified by Ca^{2+} release from IP_3- and/or caffeine-insensitive stores. First, $[Ca^{2+}]_i$ spiking continued in the presence of TG and CPA (see Figures 6A and 6B), which are thought to release Ca^{2+} from IP_3-sensitive organelles (Foskett and Wong, 1992). Second, ionomycin releases additional Ca^{2+} following depletion of stores with TG, CPA, and/or caffeine, suggesting that additional stores are available to release Ca^{2+} in the presence of these drugs (see Figure 6A and Figure 7A). Third, ryanodine reduced the amplitude of $[Ca^{2+}]_i$ transients in all growth cones examined (see Figure 7C). If repetitive release and reuptake of Ca^{2+} from an intracellular store contribute to $[Ca^{2+}]_i$ spikes in growth cones, the refilling of the stores must occur either by a TG/CPA-insensitive Ca^{2+}–ATPase or by a mechanism that does not involve Ca^{2+}–ATPase activity.

Physiological Relevance of $[Ca^{2+}]_i$ Spikes in Growth Cones

Many previous studies have implicated $[Ca^{2+}]_i$ as a regulator of neurite outgrowth (Anglister et al., 1982; Suarez-Isla et al., 1984; Cohan and Kater, 1986; Connor, 1986; Mattson and Kater, 1987; Silver et al., 1989, 1990; Fields et al., 1990; Bedlack et al., 1992; Davenport and Kater, 1992; however, for exceptions see Campenot and Draker, 1989; Tolkovsky et al., 1990; Garyantes and Regehr, 1992), leading to the notion that alteration of growth cone $[Ca^{2+}]_i$, above or below an optimum range, inhibits neurite outgrowth (Ca^{2+} "set point" hypothesis reviewed in Kater and Mills, 1991). Consistent with this theory are studies showing that agents which elevate $[Ca^{2+}]_i$ stop neurite outgrowth (Haydon et al., 1984; Cohan and Kater, 1986; Mattson et al., 1988a; Lankford and Letourneau, 1989; Fields et al., 1990), and it is believed that environmental factors may operate in this way in vivo to halt growth cone advance in preparation for synapse formation, turning, and branching (Zoran et al., 1993; Snow et al., 1994). Interestingly, growth cones can eventually adapt to prolonged elevation of $[Ca^{2+}]_i$ and resume growth with an altered Ca^{2+} set point (Fields et al., 1993). Furthermore, chronically stimulated growth cones become resistant to the inhibitory effects of subsequent stimulation. Transient changes in $[Ca^{2+}]_i$ may allow growth cone activity to be regulated by brief elevations of $[Ca^{2+}]_i$ above a set point, without inducing adaptation in the homeostatic mechanisms. Therefore, $[Ca^{2+}]_i$ spiking could regulate growth cone migration during the entire period of neurite outgrowth and synapse formation.

Consistent with previous findings, our results indicate that spontaneous $[Ca^{2+}]_i$ spikes in growth cones slow migration. We compared the rate of migration of 9 growth cones before and after 16 $[Ca^{2+}]_i$ transients and found that neurite outgrowth was significantly reduced immediately and transiently following $[Ca^{2+}]_i$ spikes (see Figure 8). Furthermore, growth cone migration recovered to a near prespike rate usually within 10 min after the spike peak. Although not quantified, the degree and duration of slowing appeared to be dependent on both the amplitude and duration of the $[Ca^{2+}]_i$ transient. Using phase-contrast timelapse microscopy, we examined the behavior of many more growth cones during shifts from 2 to 20 mM $(Ca^{2+})_o$. The average rate of migration of growth cones in 20 mM $(Ca^{2+})_o$ decreased to 33% of the rate in 2 mM $(Ca^{2+})_o$. These findings are consistent with the fact that 20 mM $(Ca^{2+})_o$ increased the percentage of growth cones that spike, and that $[Ca^{2+}]_i$ spiking is associated with a reduced rate of migration. As an alternative, 20 mM $(Ca^{2+})_o$ may reduce the rate of neurite outgrowth by increasing the baseline $[Ca^{2+}]_i$ of the growth cone. As indicated in Table 1, elevating $[Ca^{2+}]_o$ to 20 mM increased the baseline $[Ca^{2+}]_i$ of growth cones by an average of 41 ± 28 nM, which may be sufficient to reduce growth cone motility (Lankford and Letourneau, 1991). However, it was noted that 31% of growth cones showed little rate change in 20 mM $(Ca^{2+})_o$ (decreased to 82% of control), and although $[Ca^{2+}]_i$ was not measured, it is interesting to speculate that these growth cones exhibited baseline $[Ca^{2+}]_i$ changes, but no $[Ca^{2+}]_i$ transients.

$[Ca^{2+}]_i$ spiking provides several advantages to a growth cone over sustained elevation of $[Ca^{2+}]_i$. One striking feature is the clear difference between nonspike noise and the sharp, transient changes of spikes. $[Ca^{2+}]_i$ spiking enables different downstream Ca^{2+}-regulated effectors to operate with specific kinetics of activation and deactivation. This system can be further regulated by agents that lower or raise the threshold for spiking or the threshold for protein activation by Ca^{2+}. Sustained elevation of $[Ca^{2+}]_i$, on the other hand, can only encode the strength of a stimulus by the amplitude or duration of the elevated $[Ca^{2+}]_i$. The strength of a stimulus in an oscillating system can be encoded by the number or frequency of spikes. A system that relies on sustained changes in $[Ca^{2+}]_i$ is less precise and more apt to produce damaging effects when the $[Ca^{2+}]_i$ exceeds the level necessary to activate many enzymes.

Spatially localized changes in $[Ca^{2+}]_i$ may affect growth

cone behavior differently than global $[Ca^{2+}]_i$ changes (see above). Focally applied electric fields and soluble factors that locally elevate $[Ca^{2+}]_i$ have been shown to orient process outgrowth in a Ca^{2+} influx–dependent fashion (Gundersen and Barrett, 1980; Goldberg, 1988; Bedlack et al., 1992; Davenport and Kater, 1992; Zheng et al., 1994). Local elevation of $[Ca^{2+}]_i$ may direct neurite outgrowth by activating Ca^{2+}-dependent proteins that cause local reorganization of the cytoskeleton. For example, local elevation of $[Ca^{2+}]_i$ may cause a focused disruption of actin filament networks and subsequent nucleation of new actin filaments in response to Ca^{2+} binding of gelsolin and α-actinin (Stossel et al., 1985). The spontaneous $[Ca^{2+}]_i$ transients we observed in growth cones typically involved the entire growth cone; however, localized hot spots of elevated $[Ca^{2+}]_i$ often occurred (see Figure 4). In both 2 and 20 mM $(Ca^{2+})_o$, $[Ca^{2+}]_i$ hot spots apparently exceeded 1 μM, which would locally activate proteins sensitive to this concentration of Ca^{2+}. $[Ca^{2+}]_i$ hot spots within growth cones following electrical activity have been associated with local morphological changes (Silver et al., 1990). Spontaneous $[Ca^{2+}]_i$ transients within growth cones could arise locally, if Ca^{2+} currents associated with transients were locally activated. Local activation of Ca^{2+} currents may result from receptor–ligand interactions, possibly at the tips of filopodia, when growth cones encounter restricted expression of growth-influencing molecules in vivo (Davenport et al., 1993; Gomez and Letourneau, 1994).

We have observed that $[Ca^{2+}]_i$ transients in individual neurons pass down a neurite to different degrees and, in some cases, are initiated from within the neurite. Therefore, $[Ca^{2+}]_i$ spikes may influence the neurite proximal to the growth cone and could, in the shorter, newly initiated, or newly branched processes, signal back to the cell body or between growth cones. Ca^{2+} signals that reach the cell body may influence gene expression (Spitzer, 1991), while changes that are initiated within neurites could be associated with back-branching (Simon and O'Leary, 1992; Williams et al., 1993, Soc. Neurosci., abstract).

Experimental Procedures

Cell Culture

Acid-washed coverslips were mounted over 22 mm holes drilled into the bottom of 35 mm tissue culture dishes. Each dish was UV-sterilized for 1–2 hr. Human plasma fibronectin (25 μg/ml; generous gift of Dr. J. McCarthy, University of Minnesota) was coated onto each coverslip for 6–12 hr at room temperature. Each coverslip was washed extensively with PBS (pH 7.1) prior to cell seeding.

DRGs of the lumbosacral enlargement were dissected from embryonic day 8–11 white Leghorn chicken embryos and dissociated with 0.25% crude trypsin in Ca^{2+}- and Mg^{2+}-free PBS (pH 7.89) as described previously (Ludueña, 1973). Dissociated cells were suspended in serum-free medium consisting of 10 mM HEPES-buffered F14 medium (special order; GIBCO Laboratories, Grand Island, NY) supplemented with 2 mM L-glutamate, 5 ng/ml sodium selenite, 5 ng/ml sodium pyruvate, 5 mM phosphocreatine, 20 nM progesterone, 5 μg/ml insulin, 100 μg/ml transferrin (all from Sigma Chemical Co., St. Louis, MO), and 15–50 ng/ml 2.5s nerve growth factor (β-NGF; R & D systems, Minneapolis, MN). An antibiotic/antimycotic solution (penicillin, streptomycin, fungizone; Sigma) was also added. Approximately 1.0×10^5 to 2.0×10^5 cells were seeded onto each coverslip in 1.0 ml of growth medium and incubated in a humidified air chamber at 40°C for at least 6 hr. This plating density typically allowed us to observe growth cones that were isolated from contact with neighboring cells; however, in some cases growth cones did contact one another or, more commonly, were in contact with other neurites. No obvious differences in $[Ca^{2+}]_i$ homeostasis was recognized for growth cones in isolation as compared with those in contact with other cells.

Videomicroscopy

Following incubation, a culture dish was placed on an inverted microscope (Diaphot; Nikon Inc., Garden City, NY) under an air curtain incubator (ASI 400; Carl Zeiss, Inc., Thornwood, NY) keeping the medium at a constant 40°C. For behavioral studies, growth cones were monitored with phase-contrast optics. Images were captured using a 10× phase 1 air objective (Nikon), a Newvicon video camera (NC-65; Dage-MTI, Inc., Michigan City, IN), and image enhancement software (Image 1; Universal Imaging, Inc., West Chester, PA) running on a 486/33 computer system (Gateway 2000, North Sioux City, SD). Images, viewed with a video monitor (Trinitron; Sony Corp. of America, New York, NY), were recorded every minute with an optical disc recorder (TQ-2026F; Panasonic Industrial Computers, Secaucus, NJ).

Fura 2 Loading

The $[Ca^{2+}]_i$ of growth cones, nerve cell bodies, and nonneuronal cells (judged morphologically by large, flattened lamellar surface and no neurites) was estimated using the Ca^{2+} indicator Fura 2 (Molecular Probes, Eugene, OR). Cells were loaded with the cell-permeant, acetoxymethyl ester form of Fura 2 by incubating 8- to 24-hr-old cultures, which had obvious process outgrowth, with 2–5 μM Fura 2, diluted in culture medium, for 30–45 min at 40°C. The cells were subsequently washed six times with warm culture medium, and the dye was allowed to de-esterify for an additional 30–60 min in the humidified chamber. The Fura 2 loading solutions were made from 1 mM stock solutions of Fura 2 diluted in dimethylsulfoxide (Sigma).

Ca^{2+} Measurements

All Ca^{2+} measurements were made using a Nikon Diaphot inverted microscope (Nikon) equipped with a 100 W HBO epiillumination light source. A software-driven (Image 1/Fluor; Universal Imaging, Inc.) filter wheel (AZI; Atlantex and Zieler Instrument Corp., Avon, MA) switched excitation wavelengths between 350 ± 5 nm and 380 ± 5 nm. Experiments examining the effect of Ni^{2+}, La^{3+}, and caffeine on cell-free Fura 2 fluorescence were performed on glass coverslips using a 359 ± 2 nm excitation filter, as well as the 350 and 380 nm filters, to excite Fura 2 at its isosbestic point. To prevent UV photodamage of the growth cones and photobleaching of the dye, quartz UV-grade neutral density filters of optical density totaling 2.1 and 2.3 were placed in front of the 350 and 380 nm excitation filters, respectively. All optical filters were obtained from Omega Optical (Brattleboro, VT). Excitation and emission wavelengths were separated with a 400 nm dichroic mirror (Nikon), and cells were observed with a Zeiss 100× phase-contrast oil-immersion neofluor objective (NA = 1.3). Images were captured using a intensified CCD camera (Paultek Imaging, Nevada City, CA) connected to a 486/33 computer system (Gateway 2000), running Image 1/AT digital image processing software (Universal Imaging, Inc.) that was set to average 16 frames, correct for background fluorescence (based on a cell-free portion of the culture dish), and record the subsequent image to an optical disc (TQ-2026F). Upon completion of the experiment, the recorded images were ratioed using the Image 1/AT software, and the average $[Ca^{2+}]_i$ within a user-defined region of the growth cone, cell body, or nonneuronal cell was estimated using a calibrated scale. Free $[Ca^{2+}]_i$ was estimated using the equation of Grynkiewicz et al. (1985):

$$[Ca^{2+}]_i = K_D\beta[(R - R_{min})/R_{max} - R)],$$

where R is the 350:380 nm fluorescence emission ratio. The maximum ratio (R_{max}), minimum ratio (R_{min}), and β value (emission ratio of free to bound Fura 2 at 380 nm) were determined in ionomycin-permeabilized cell bodies in Ca^{2+}-free (1 mM EGTA) and saturating Ca^{2+} (10 mM Ca^{2+}) media. For our microscope, R_{min} is 0.47, R_{max} is 3.9, and β is 4.84. The dissociation constant of Fura 2 for Ca^{2+} (K_D) was assumed to be 224 nM (Grynkiewicz et al., 1985).

Solution Changes

After Fura 2 loading and de-esterification, culture dishes were removed from the incubator, and 300 μm thick spacers were placed at each corner, upon which a second coverslip was placed. The chamber was sealed along its length using high vacuum grease (Dow Corning Corp., Midland, MI). Both ends of the "coverslip sandwich" were left open for exchange of solutions. This arrangement produced a chamber volume of ~250 μl and allowed us to exchange solutions rapidly 3–4 times this volume. The culture dish was then placed on the microscope stage and kept at a constant 40°C with an air-curtain incubator (ASI 400; Zeiss).

In our initial experiments, neuronal growth cones migrating in F14 medium containing 2 mM $(Ca^{2+})_o$ were imaged every 30 s; however, in all subsequent experiments images were captured every 10 s. Most experiments were conducted in a modified Ringer solution that contained no phosphate, carbonate, or sulfate anions, to prevent precipitation of Ca^{2+} and other polyvalent cations. The basic medium was composed of the following: 10 mM HEPES, 140 mM NaCl, 5.6 mM KCl, 2 mM $CaCl_2$, 1 mM $MgCl_2$, 5.5 mM glucose (all from Sigma), and 15 ng/ml β-NGF. The concentration of Ca^{2+} in this solution was varied from 0 to 20 mM by removing or adding more $CaCl_2$. Unless otherwise noted, Ca^{2+}-free solutions did not contain EGTA. The various pharmacological agents used were brought to their final dilution in the appropriate Ca^{2+}-containing medium and warmed to 40°C prior to application.

TG and CPA were purchased from Biomol Research Laboratories (Plymouth Meeting, PA); ionomycin, caffeine, EGTA, and verapamil, from Calbiochem (San Diego, CA); ryanodine, from Research Biochemicals International (Natick, MA); ω-conotoxin, $NiCl_2$, and $LaCl_3$, from Sigma.

Quantitative Analysis

Estimates of the average $[Ca^{2+}]_i$ within a user-defined region of growth cones, neurites, cell bodies, and nonneuronal cells were logged to text files, using Image 1/Fluor software, during OMDR replay of completed experiments. $[Ca^{2+}]_i$ spikes were scored as events if the $[Ca^{2+}]_i$ increased transiently ($\leq$3 min duration) by $\geq$100 nM over baseline. Growth cone migration rate was determined by measuring the leading margin of fluorescent or phase-contrast growth cones at successive time points using micrometer-calibrated Image 1 software. For statistical analysis and graphics, text files were transferred to a Macintosh-based system (Quadra 950; Apple Computer, Inc., Cupertino, CA) running spreadsheet (Excel; Microsoft Corp., Redmond, WA) and graphics software (Cricket graph; Computer Associates International, Inc., Islandia, NY). For image reproduction, ratio images were transferred to a Macintosh-based image processing program (Photoshop; Adobe Systems, Inc., Mountain View, CA) and printed using a color laser imager (Pictrography 3000; Fugi, Elmsford, NY). To determine statistical significance, unpaired (equal or unequal variance) Student's t tests were performed (paired test where indicated) using SAS (SAS Institute, Inc., Cary, NC) or Statview II (Abacus Concepts, Inc., Berkeley, CA) software.

Acknowledgments

This research was supported by National Institutes of Health predoctoral training grant EY07133 (T. M. G), NIH grants HD19950 (T. M. G. and P. C. L.) and EY06331 (D. M. S.), and a grant from the American Paralysis Association (P. C. L. and D. M. S.).

The costs of publication of this article were defrayed in part by the payment of page charges. This article must therefore be hereby marked *"advertisement"* in accordance with 18 USC Section 1734 solely to indicate this fact.

Received October 5, 1995; revised March 18, 1995.

References

Anglister, L., Farber, I. C., Shahar, A., and Grinvald, A. (1982). Localization of voltage-sensitive calcium channels along developing neurites: their possible role in regulating neurite elongation. Dev. Biol. *94*, 351–365.

Ascher, P., Bregestovski, P., and Nowak, L. (1988). N-methyl-D-aspartate-activated channels of mouse central neurones in magnesium-free solutions. J. Physiol. *399*, 207–226.

Augustine, G. J., Charlton, M. P., and Smith, S. J. (1987). Calcium action in synaptic transmitter release. Annu. Rev. Neurosci. *10*, 633–694.

Bandtlow, C. E., Schmidt, M. F., Hassinger, T. D., Schwab, M. E., and Kater, S. B. (1993). Role of intracellular calcium in NI-35-evoked collapse of neuronal growth cones. Science *259*, 80–83.

Bean, B. P. (1989). Classes of calcium channels in vertebrate cells. Annu. Rev. Physiol. *51*, 367–384.

Bedlack, R. S., Jr., Wei, M.-d., and Loew, L. M. (1992). Localized membrane depolarizations and localized calcium influx during electric field–guided neurite growth. Neuron *9*, 393–403.

Bengtsson, T., Jaconi, M. E., Gustafson, M., Magnusson, K. E., Theler, J. M., Lew, D. P., and Stendahl, O. (1993). Actin dynamics in human neutrophils during adhesion and phagocytosis is controlled by changes in intracellular free calcium. Eur. J. Cell Biol. *62*, 49–58.

Benham, C. D., and Tsien, R. W. (1987). A novel receptor-operated Ca^{2+}-permeable channel activated by ATP in smooth muscle. Nature *328*, 275–278.

Berridge, M. J. (1993). Inositol triphosphate and calcium signalling. Nature *361*, 315–325.

Berridge, M. J., Cobbold, P. H., and Cuthbertson, K. S. (1988). Spatial and temporal aspects of cell signalling. Philos. Trans. R. Soc. Lond. (B) *320*, 325–343.

Billger, M., Wallin, M., and Karlsson, J. O. (1988). Proteolysis of tubulin and microtubule-associated proteins 1 and 2 by calpain I and II. Difference in sensitivity of assembled and disassembled microtubules. Cell Calcium *9*, 33–44.

Bixby, J. L. (1989). Protein Kinase C is involved in laminin stimulation of neurite outgrowth. Neuron *3*, 287–297.

Brehm, P., and Eckert, R. (1978). Calcium entry leads to inactivation of calcium channel in *Paramecium*. Science *202*, 1203–1206.

Campenot, R. B., and Draker, D. D. (1989). Growth of sympathetic nerve fibers in culture does not require extracellular calcium. Neuron *3*, 733–743.

Clementi, E., Scheer, H., Zacchetti, D., Fasolato, C., Pozzan, T., and Meldolesi, J. (1992). Receptor-activated Ca^{2+} influx: two independently regulated mechanisms of influx stimulation coexist in neurosecretory PC12 cells. J. Biol. Chem. *267*, 2164–2172.

Cohan, C. S., and Kater, S. B. (1986). Suppression of neurite elongation and growth cone motility by electrical activity. Science *232*, 1638–1640.

Connor, J. A. (1986). Digital imaging of free calcium changes and of spatial gradients in growing processes in single, mammalian central nervous system cells. Proc. Natl. Acad. Sci. USA *83*, 6179–6183.

Cunningham, C. C., Stossel, T. P., and Kwiatkowski, D. J. (1991). Enhanced motility in NIH 3T3 fibroblasts that overexpress gelsolin. Science *251*, 1233–1236.

Davenport, R. W., and Kater, S. B. (1992). Local increases in intracellular calcium elicit local filopodial responses in Helisoma neuronal growth cones. Neuron *9*, 405–416.

Davenport, R. W., Dou, P., Rehder, V., and Kater, S. B. (1993). A sensory role for neuronal growth cone filopodia. Science *361*, 721–724.

Demaurex, N., Lew, D. P., and Krause, K. H. (1992). Cyclopiazonic acid depletes intracellular Ca^{2+} stores and activates an influx pathway for divalent cations in HL-60 cells. J. Biol. Chem. *267*, 2318–2324.

Doherty, P., Furness, J., Williams, E. J., and Walsh, F. S. (1994). Neurite outgrowth stimulated by the tyrosine kinase inhibitor herbimycin A requires activation of tyrosine kinases and protein kinase C. J. Neurochem. *62*, 2124–2131.

Fabiato, A. (1983). Calcium-induced release of calcium from cardiac sarcoplasmic reticulum. Am. J. Physiol. *245*, C1–C14.

Fewtrell, C. (1993). Ca^{2+} oscillations in non-excitable cells. Annu. Rev. Physiol. *55*, 427–454.

Fields, R. D., Neale, E. A., and Nelson, P. G. (1990). Effects of patterned electrical activity on neurite outgrowth from mouse sensory neurons. J. Neurosci. *10*, 2950–2964.

Fields, R. D., Guthrie, P. B., Russell, J. T., Kater, S. B., Malhotra, B. S., and Nelson, P. G. (1993). Accomodation of mouse DRG growth cones to electrically induced collapse: kinetic analysis of calcium transients and set-point theory. J. Neurobiol. *24*, 1080–1098.

Foskett, J. K., and Wong, D. (1992). Calcium oscillations in parotid acinar cells induced by microsomal Ca^{2+}-ATPase inhibition. Am. J. Physiol. *262*, C656–C663.

Foskett, J. K., Roifman, C. M., and Wong, D. (1991). Activation of calcium oscillations by thapsigargin in parotid acinar cells. J. Biol. Chem. *266*, 14535–14538.

Fox, A. P., Nowycky, M. C., and Tsien, R. W. (1987). Kinetic and pharmacological properties distinguishing three types of calcium currents in chick sensory neurones. J. Physiol. *394*, 149–172.

Friel, D. D., and Tsien, R. W. (1992). Phase-dependent contributions from Ca^{2+} entry and Ca^{2+} release to caffeine-induced $[Ca^{2+}]_i$ oscillations in bullfrog sympathetic neurons. Neuron *8*, 1109–1125.

Garyantes, T. K., and Regehr, W. G. (1992). Electrical activity increases growth cone calcium but fails to inhibit neurite outgrowth from rat sympathetic neurons. J. Neurosci. *12*, 96–103.

Giannini, G., Clementi, E., Ceci, R., Marziali, G., and Sorrentino, V. (1992). Expression of a ryanodine receptor-Ca^{2+} channel that is regulated by TGF-β. Science *257*, 91–94.

Goldberg, D. J. (1988). Local role of Ca^{2+} in formation of veils in growth cones. J. Neurosci. *8*, 2596–2605.

Gomez, T. M., and Letourneau, P. C. (1994). Filopodia initiate choices made by sensory neuron growth cones at laminin/fibronectin borders *in vitro*. J. Neurosci. *14*, 5959–5972.

Grynkiewicz, G., Poenie, M., and Tsien, R. Y. (1985). A new generation of Ca^{2+} indicators with greatly improved fluorescence properties. J. Biol. Chem. *260*, 3440–3450.

Gundersen, R. W., and Barrett, J. N. (1980). Characterization of the turning response of dorsal root neurites toward nerve growth factor. J. Cell Biol. *87*, 546–554.

Gurney, A. M., Charnet, P., Pye, J. M., and Nargeot, J. (1989). Augmentation of cardiac calcium current by flash photolysis of intracellular caged-Ca^{2+} molecules. Nature *341*, 65–68.

Haydon, P. G., McCobb, D. P., and Kater, S. B. (1984). Serotonin selectively inhibits growth cone motility and synaptogenesis of specific identified neurons. Science *226*, 561–564.

Hua, S.-Y., Tokimasa, T., Takasawa, S., Furuya, Y., Nohmi, M., Okamoto, H., and Kuba, K. (1994). Cyclic ADP-ribose modulates Ca^{2+} release channels for activation by physiological Ca^{2+} entry in bullfrog sympathetic neurons. Neuron *12*, 1073–1079.

Hughes, A. D., Hering, S., and Bolton, T. B. (1990). The action of caffeine on inward barium current through voltage-dependent calcium channels in single rabbit ear artery cells. Pflügers Arch. *416*, 462–466.

Imagawa, T., Smith, J. S., Coronado, R., and Campbell, K. P. (1987). Purified ryanodine receptor from skeletal muscle sarcoplasmic reticulum is the Ca^{2+}-permeable pore of the calcium release channel. J. Biol. Chem. *262*, 16636–16643.

Kater, S. B., and Mills, L. R. (1991). Regulation of growth cone behavior by calcium. J. Neurosci. *11*, 891–899.

Kater, S. B., Mattson, M. P., Cohan, C., and Connor, J. (1988). Calcium regulation of the neuronal growth cone. J. Neurosci. *11*, 891–899.

Keith, C. K., Di Poala, M., Maxfield, F., and Shelanski, M. (1983). Microinjection of calcium calmodulin causes local depolymerization of microtubules. J. Cell Biol. *97*, 1918–1924.

Kojima, I., Mogami, H., and Ogata, E. (1992). Oscillation of cytoplasmic free calcium concentration induced by insulin-like growth factor I. Am. J. Physiol. *262*, E307–E311.

Kuba, K., and Nishi, S. (1976). Rhythmic hyperpolarization and depolarization of sympathetic ganglion cells induced by caffeine. J. Neurophysiol. *39*, 547–563.

Kuba, K., and Takeshita, S. (1981). Simulation of intracellular Ca^{2+} oscillation in a sympathetic neurone. J. Theor. Biol. *93*, 1009–1031.

Lahof, A. M., Quillan, M., Dan, Y., and Poo, M.-m. (1992). Asymmetric modulation of cytosolic cAMP activity induces growth cone turning. J. Neurosci. *12*, 1253–1261.

Lai, F. A., Misra, M., Xu, L., Smith, H. A., and Meissner, G. (1989). The ryanodine receptor–Ca^{2+} release channel complex of skeletal muscle sarcoplasmic reticulum. Evidence for a cooperatively coupled, negatively charged homotetramer. J. Biol. Chem. *264*, 16776–16785.

Lankford, K. L., and Letourneau, P. C. (1989). Evidence that calcium may control neurite outgrowth by regulating the stability of actin filaments. J. Cell Biol. *109*, 1229–1243.

Lankford, K. L., and Letourneau, P. C. (1991). Roles of actin filaments and three second-messenger systems in short-term regulation of chick dorsal root ganglion neurite outgrowth. Cell Motil. Cytoskel. *20*, 7–29.

Laskey, R. E., Adams, D. J., Cannell, M., and van Breemen, C. (1992). Calcium entry–dependent oscillations of cytoplasmic calcium concentration in cultured endothelial cell monolayers. Proc. Natl. Acad. Sci. USA *89*, 1690–1694.

Lee, H. C. (1993). Potentiation of calcium- and caffeine-induced calcium release by cyclic ADP-ribose. J. Biol. Chem. *268*, 293–299.

Letourneau, P. C. (1981). Immunocytochemical evidence for colocalization in neurite growth cones of actin and myosin and their relationship to cell-substratum adhesions. Dev. Biol. *85*, 113–122.

Letourneau, P. C., and Cypher, C. (1991). Regulation of growth cone motility. Cell Motil. Cytoskel. *20*, 267–271.

Lewis, R. S., and Cahalan, M. D. (1989). Mitogen-induced oscillations of cytoplasmic Ca^{2+} and transmembrane Ca^{2+} current in human leukemic T cells. Cell Regul. *1*, 99–112.

Lipscombe, D., Madison, D. V., Poenie, M., Reuter, H., Tsien, R. W., and Tsien, R. Y. (1988a). Imaging of cytosolic Ca^{2+} transients arising from Ca^{2+} stores and Ca^{2+} channels in sympathetic neurons. Neuron *1*, 355–365.

Lipscombe, D., Madison, D. V., Poenie, M., Reuter, H., Tsien, R. W., and Tsien, R. Y. (1988b). Spatial distribution of calcium channels and cystolic calcium transients in growth cones and cell bodies of sympathetic neurons. Proc. Natl. Acad. Sci. USA *85*, 2398–2402.

Ludueña, M. A. (1973). The growth of spinal ganglion neurons in serum-free medium. Dev. Biol. *33*, 470–476.

Marban, E., and Tsien, R. W. (1982). Enhancement of calcium current during digitalis inotropy in mammalian heart: positive feed-back regulation by intracellular calcium? J. Physiol. *329*, 589–614.

Martin, C., Dacquet, C., Mironneau, C., and Mironneau, J. (1989). Caffeine-induced inhibition of calcium channel current in cultured smooth cells from pregnant rat myometrium. Br. J. Pharmacol. *98*, 493–498.

Mattson, M. P., and Kater, S. B. (1987). Calcium regulation of neurite elongation and growth cone motility. J. Neurosci. *7*, 4034–4043.

Mattson, M. P., Dou, P., and Kater, S. B. (1988a). Outgrowth-regulating actions of glutamate in isolated hippocampal pyramidal neurons. J. Neurosci. *8*, 2087–2100.

Mattson, M. P., Taylor-Hunter, A., and Kater, S. B. (1988b). Neurite outgrowth in individual neurons of a neuronal population is differentially regulated by calcium and cyclic AMP. J. Neurosci. *8*, 1704–1711.

McPherson, P. S., Kim, Y.-K., Valdivia, H., Knudson, C. M., Takekura, H., Franzini-Armstrong, C., Coronado, R., and Campbell, K. P. (1991). The brain ryanodine receptor: a caffeine-sensitive calcium release channel. Neuron *7*, 17–25.

Meyer, T., and Stryer, L. (1991). Calcium spiking. Annu. Rev. Biophys. Biophys. Chem. *20*, 153–174.

Neyses, L., Reinlib, L., and Carafoli, E. (1985). Phosphorylation of the Ca^{2+}-pumping ATPase of heart sarcolemma and erythrocyte plasma membrane by the cAMP-dependent protein kinase. J. Biol. Chem. *18*, 10283–10287.

Noack, T. H., Deitmer, P., and Golenhofen, K. (1990). Features of a calcium independent, caffeine sensitive outward current in single

smooth muscle cells from guinea pig protal vein. Pflügers Arch. *416*, 467–469.

Nohmi, M., Hua, S. Y., and Kuba, K. (1992). Basal Ca^{2+} and the oscillation of Ca^{2+} in caffeine-treated bullfrog sympathetic neurones. J. Physiol. *??*, 513–528.

Rehder, V., and Kater, S. B. (1992). Regulation of neuronal growth cone filopodia by intracellular calcium. J. Neurosci. *12*, 3175–3186.

Rosenmund, C., and Westbrook, G. L. (1993). Calcium-induced actin depolymerization reduces NMDA channel activity. Neuron *10*, 805–814.

Rousseau, E., and Meissner, G. (1989). Single cardiac sarcoplasmic reticulum Ca^{2+}-release channel: activation by caffeine. Am. J. Physiol. *256*, H328–H333.

Schilling, W. P., Rajan, L., and Strobl-Jager, E. (1989). Characterization of the bradykinin-stimulated calcium influx pathway of cultured vascular endothelial cells. J. Biol. Chem. *264*, 12838–12848.

Seidler, N. W., Jona, I., Vegh, M., and Martonosi, A. (1989). Cyclopiazonic acid is a specific inhibitor of the Ca^{2+}-ATPase of sarcoplasmic reticulum. J. Biol. Chem. *264*, 17816–17823.

Shea, T. B., Beermann, M. L., and Nixon, R. A. (1991). Multiple proteases regulate neurite outgrowth in NB2a/dl neuroblastoma cells. J. Neurochem. *56*, 842–851.

Shibuya, I., and Douglas, W. W. (1992). Calcium channels in rat melanotrophs are permeable to manganese, cobalt, cadmium, and lanthanum, but not to nickel: evidence provided by fluorescence changes in Fura-2-loaded cells. Endocrinology *131*, 1936–1941.

Silver, R. A., Lamb, A. G., and Bolsover, S. R. (1989). Elevated cytosolic calcium in the growth cone inhibits neurite elongation in neuroblastoma cells: correlation of behavioral states with cytosolic calcium concentration. J. Neurosci. *9*, 4007–4020.

Silver, R. A., Lamb, A. G., and Bolsover, S. R. (1990). Calcium hotspots caused by L-channel clustering promote morphological changes in neuronal growth cones. Nature *343*, 751–754.

Simon, D. K., and O'Leary, D. D. M. (1992). Responses of retinal axons in vivo and in vitro to position-encoding molecules in the embryonic superior colliculus. Neuron *9*, 977–989.

Smith, S. J. (1988). Neuronal cytomechanics: the actin-based motility of growth cones. Science *242*, 708–715.

Snow, D. M., Atkinson, P., Hassinger, T., Kater, S. B., and Letourneau, P. C. (1994). Growth cone intracellular calcium levels are elevated upon contact with sulfated proteoglycans. Dev. Biol. *166*, 87–100.

Sobue, K., and Kanda, K. (1989). α-Actinins, calspectin (brain spectrin or fodrin), and actin participate in adhesion and movement of growth cones. Neuron *3*, 311–319.

Spitzer, N. C. (1991). A developmental handshake: neuronal control of ionic currents and their control of neuronal differentiation. J. Neurobiol. *22*, 659–673.

Stossel, T. P., Chaponnier, C., Ezzell, R. M., Hartwig, J. H., Janmey, P. A., Kwiatkowski, D. J., Lind, S. E., Smith, D. B., Southwick, F. S., Yin, H. L., and Zaner, K. S. (1985). Nonmuscle actin-binding proteins. Annu. Rev. Cell Biol. *1*, 353–402.

Suarez-Isla, B. A., Pelto, D. J., Thompson, J. M., and Rapoport, S. T. (1984). Blockers of calcium permeability inhibit neurite extension and formation of neuromuscular synapses in cell culture. Exp. Brain Res. *14*, 263–270.

Suematsu, E., Hirata, M., and Kuriyama, H. (1984). Effects of cAMP- and cGMP-dependent protein kinases, and calmodulin on Ca^{2+} uptake by highly purified sarcolemmal vesicles of vascular smooth muscle. Biochim. Biophys. Acta *773*, 83–90.

Thastrup, O. P., Cullen, P. J., Drobak, B. K., Hanley, M. R., and Dawson, A. P. (1990). Thapsigargin, a tumor promoter, discharges intracellular Ca^{2+} stores by specific inhibition of the endoplasmic reticulum Ca^{2+}-ATPase. Proc. Natl. Acad. Sci. USA *87*, 2466–2470.

Thayer, S. A., Hirning, L. D., and Miller, R. J. (1988a). The role of caffeine-sensitive calcium stores in the regulation of the intracellular free calcium concentration in rat sympathetic neurons *in vitro*. Mol. Pharmacol. *34*, 664–673.

Thayer, S. A., Perney, T. M., and Miller, R. J. (1988b). Regulation of calcium homeostasis in sensory neurons by bradykinin. J. Neurosci. *8*, 4089–4097.

Tolkovsky, A. M., Walker, A. E., Murrell, R. D., and Suidan, H. S. (1990). Ca^{2+} transients are not required as signals for long-term neurite outgrowth from cultured sympathetic neurons. J. Cell Biol. *110*, 1295–1306.

Tsien, R. W., and Tsien, R. Y. (1990). Calcium channels, stores, and oscillations. Annu. Rev. Cell Biol. *6*, 715–760.

Tsien, R. W., Lipscombe, D., Madison, D. V., Bley, K. R., and Fox, A. P. (1988). Multiple types of neuronal calcium channels and their selective modulation. Trends Neurosci. *11*, 431–438.

Volberg, T., Geiger, B., Kartenbeck, J., and Franke, W. W. (1986). Changes in membrane–microfilament interaction in intercellular adherens junctions upon removal of extracellular Ca^{2+} ions. J. Cell Biol. *102*, 1832–1842.

Wakui, M., Osipchuk, Y. V., and Petersen, O. H. (1990). Receptor-activated cytoplasmic Ca^{2+} spiking mediated by inositol trisphosphate is due to Ca^{2+}-induced Ca^{2+} release. Cell *63*, 1025–1032.

Williams, E. J., Doherty, P., Turner, G., Reid, R. A., Hemperly, J. J., and Walsh, F. S. (1992). Calcium influx into neurons can solely account for cell contact–dependent neurite outgrowth stimulated by transfected L1. J. Cell Biol. *119*, 883–892.

Woods, N. M., Cuthbertson, K. S., and Cobbold, P. H. (1986). Repetitive transient rises in cytoplasmic free calcium in hormone-stimulated hepatocytes. Nature *319*, 600–602.

Wu, D. Y., and Goldberg, D. J. (1993). Regulated tyrosine phosphorylation at the tips of growth cone filopodia. J. Cell Biol. *123*, 653–664.

Zheng, J. Q., Felder, M., Conner, J. A., and Poo, M.-m. (1994). Turning of nerve growth cones induced by neurotransmitters. Nature *368*, 140–144.

Zoran, M. J., Funte, L. R., Kater, S. B., and Haydon, P. G. (1993). Neuron–muscle contact changes presynaptic resting calcium setpoint. Dev. Biol. *158*, 163–171.